

# MATHEMATICAL MODEL USING MACROSCOPIC AND MICROSCOPIC SCALES OF AN ELECTRICAL ARC DISCHARGE THROUGH A POROUS MEDIUM IN HBC FUSES

Rochette David<sup>(1)</sup>, Clain Stéphane<sup>(2)</sup> and Bussière William<sup>(3)</sup>

LAEPT CNRS UMR 6069 <sup>(1,3)</sup>, Phys. Bât. 5 – 24, Av. des Landais – F63177 AUBIERE CEDEX FRANCE,  
david.ROCHETTE@laept.univ-bpclermont.fr<sup>(1)</sup>, william.BUSSIERE@laept.univ-bpclermont.fr<sup>(3)</sup>  
LMA CNRS UMR 6620 <sup>(2)</sup>, 24, Av. des Landais – F63177 AUBIERE CEDEX FRANCE,  
stephane.CLAIN@math.univ-bpclermont.fr<sup>(2)</sup>

**Abstract:** We introduce a model to describe the mechanical interaction and the energy transfer mechanisms from arc column toward to porous medium occurring in the HBC fuse. The model is built on a macroscopic and microscopic approach in order to evaluate more accurately the thermal evolution of the solid phase and the vaporization and condensation processes of the silica sand. We consider a thermal model at the scale of a sand grain to determine the temperature evolution of the plasma and the sand grains and the mass transfer between the two phases. The gas flow is based on the compressible homogenized Euler equations with two species (air and silica vapours) coupled with a porous media model taking into account the mechanical interaction and the porosity variation. The governing equations are discretized following a finite volume scheme coupled with a fractional step technique. We obtain a realist evaluation of the pressure and the temperature as well as the vaporization and condensation areas in the fuse.

**Keywords:** H.B.C. fuse, porous media, heat transfer, Darcy's and Forchheimer's laws, macro/micro scales, finite volume.

## 1. Introduction

The process in the HBC fuse involves a compressible gas flow from low to high speed through a porous medium, the presence of important exchanges of energy by heat transfer between arc plasma and silica sand, the creation and the condensation of gaseous material. To describe the evolution of physical parameters such that the velocity, pressure and temperature of the gas, we use the homogenized Euler equations taking into account the presence of a porous medium since the morphology of silica grains influences the arc behaviour [1, 2]. The mechanical interaction between gas and silica sand is governed by the Darcy law which represents the viscous friction and the Forchheimer law which represents the inertial and turbulence friction. A large part of the energy contained in the arc plasma is transmitted to the porous medium. To describe the interfacial heat transfer and the mass transfer, we use a pore description named microscopic modelling of the heat transfer [3]. Our modelling consists in representing a sand grain and a pore by a simplified two-dimensional geometry. From the energy point of view, we assimilate the porous medium as a succession of gas and material layers of thickness  $R$  representative of the grain size [4]. We impose that the ratio between the solid and the fluid layer is equal to the porosity. We therefore obtain a two-dimensional model where  $(Ox)$  is the principal convection axe of the previous one-dimensional problem and  $(Oy)$  is the pore axe to represent the

thermal distribution in the grain sand. For any position in the fuse, the porous medium is described following the vertical axe by  $\bar{T}(x, y, t)$  on the interval  $[0, (1-\phi)R]$  where  $R$  is the characteristic scale of a grain and  $\phi$  is the medium porosity. The volume occupied at the micro scale by the gas and the solid phases are respectively  $\Omega_g = [(1-\phi)R, R]$  and  $\Omega_s = [0, (1-\phi)R]$ . We assume each volume as one as shown in figure 1.

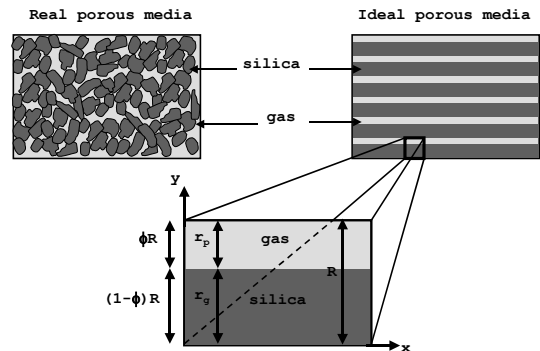


Fig. 1: Microscopic schematic description of a silica grain and a pore.

In section 2, we introduce the mathematical model compounded of a microscopic thermal 2D model and a macroscopic gas flow 1D model. Section 3 is devoted to numerical methods to obtain an approximated solution, we use a finite volume scheme based on a fractional step technique. In section 4, the geometry of the problem is given and

in the last section some numerical results are presented.

## 2. Mathematical model

### 2.1. Solid-gas total energy model

The major idea is to introduce the conservation energy equation both for the gas and the solid. We use the total energy form due to the pressure variation. Let us denote by  $\bar{E}(x, y, t)$  the total energy density,  $\bar{T}(x, y, t)$  the gas or solid temperature,  $\bar{u}(x, y, t)$  and  $\bar{v}(x, y, t)$  the gas velocity in x-direction and y-direction respectively, we then have:

$$\frac{\partial \bar{E}}{\partial t} + \frac{\partial [\bar{u}(\bar{E} + \bar{P})]}{\partial x} + \frac{\partial [\bar{v}(\bar{E} + \bar{P})]}{\partial y} - \frac{\partial}{\partial x} \left( k_x(\bar{T}) \frac{\partial \bar{T}}{\partial x} \right) - \frac{\partial}{\partial y} \left( k_y(\bar{T}) \frac{\partial \bar{T}}{\partial y} \right) = S \quad (1)$$

where  $k_x(\bar{T})$  and  $k_y(\bar{T})$  are the thermal conductivities, P is the pressure and S represents the total power density injected during fuse operation.

We introduce a new assumption: due to the weak thickness of the gas pore, the gas turbulence effects involve that the temperature, energy, pressure and density of the gas are invariant following y-direction. In the solid phase, only the dissipation effects exist since the convection is null and the pressure is constant. Consequently, in the solid part, the total energy equation is rewritten in the form:

$$\frac{\partial \bar{H}}{\partial t} - \frac{\partial}{\partial x} \left( k_x(\bar{T}) \frac{\partial \bar{T}}{\partial x} \right) - \frac{\partial}{\partial y} \left( k_y(\bar{T}) \frac{\partial \bar{T}}{\partial y} \right) = S \quad (2)$$

where  $\bar{H}$  denote the total enthalpy.

In the gas phase, Eq. (1) becomes:

$$\frac{\partial \bar{E}}{\partial t} + \frac{\partial [\bar{u}(\bar{E} + \bar{P})]}{\partial x} - \frac{\partial}{\partial x} \left( k_x(\bar{T}) \frac{\partial \bar{T}}{\partial x} \right) - \frac{\partial}{\partial y} \left( k_y(\bar{T}) \frac{\partial \bar{T}}{\partial y} \right) = S \quad (3)$$

Let us a small time interval  $\Delta t$ , the splitting operator technique yields that Eq. (3) can be approximated by solving successively a one-dimensional convection equation

$$\frac{\partial \bar{E}}{\partial t} + \frac{\partial [\bar{u}(\bar{E} + \bar{P})]}{\partial x} = 0$$

and the two-dimensional conduction equation:

$$\frac{\partial \bar{H}}{\partial t} - \frac{\partial}{\partial x} \left( k_x(\bar{T}) \frac{\partial \bar{T}}{\partial x} \right) - \frac{\partial}{\partial y} \left( k_y(\bar{T}) \frac{\partial \bar{T}}{\partial y} \right) = S$$

on the small time interval.

Since we assume a gas temperature invariant following (0y), we get that the one-dimensional total energy satisfied  $E(x, t) = \bar{E}(x, y, t)$  and thus  $T(x, t) = \bar{T}(x, y, t)$ , therefore  $\partial \bar{T} / \partial y = 0$  in the gas domain. The heat transfer between the two phases allows to evaluate the mass transfer by vaporization or condensation [4].

### 2.2. Gas flow model

The one-dimensional governing equations for a single phase fluid flow in an isotropic, homogeneous porous medium based on the compressible flow Euler equations [5] can be written in the following form:

$$\frac{\partial(\rho_{si}\phi)}{\partial t} + \frac{\partial(\rho_{si}\phi u)}{\partial x} = r \quad (4)$$

$$\frac{\partial(\rho_a\phi)}{\partial t} + \frac{\partial(\rho_a\phi u)}{\partial x} = 0 \quad (5)$$

$$\frac{\partial(\rho\phi u)}{\partial t} + \frac{\partial(\rho\phi u^2 + \phi P)}{\partial x} = P \frac{\partial \phi}{\partial x} - \phi^2 \frac{\mu}{k} u - \phi^3 \beta \rho |u| \mu \quad (6)$$

$$\frac{\partial(E\phi)}{\partial t} + \frac{\partial[(E + P)\phi u]}{\partial x} = P u \frac{\partial \phi}{\partial x} \quad (7)$$

$$\frac{\partial \phi}{\partial t} = - \frac{\bar{v}_{abl} \cdot \bar{n}}{R} \quad (8)$$

where  $\rho_{si}$ ,  $\rho_a$  and  $\rho$  are respectively the silica vapours, air and gas density and  $v_{abl}$  is the ablation velocity of the solid.

In Eq. (4), the quantity  $r$  represents the material source or loss due to the vaporization or condensation of the silica sand. In Eq. (6), the expression  $\phi^2 \frac{\mu}{k} u$  represents the viscous friction

between fluid and grains silica sand where  $\mu$  is the dynamic viscosity,  $k$  is the medium permeability and the term  $\phi^3 \beta \rho |u| \mu$  is the Forchheimer flow resistance where  $\beta$  is the Forchheimer coefficient.

In addition to close the system, we use the ideal gas equation of state:

$$p = (\gamma - 1)\rho e \quad \text{with } \gamma > 1,$$

where  $\gamma$  is the ratio of specific heat and  $e$  is the specific internal energy.

### 3. Numerical method

The numerical method is based on a fractional step technique [6]. Assume that we know approximations  $\rho_{si}^n$ ,  $\rho_a^n$ ,  $u^n$ ,  $E^n$ ,  $\phi^n$  and  $T_g^n$  for the gas and  $\bar{T}^n$ ,  $\bar{H}^n$  for the solid at time  $t^n$  and let  $\Delta t$  be a small time interval.

- We first compute an approximation  $\rho_{si}^{n+1/3}$ ,  $\rho_a^{n+1/3}$ ,  $u^{n+1/3}$ ,  $E^{n+1/3}$ ,  $\phi^{n+1/3}$  and  $T_g^{n+1/3}$  solving Eqs. (4) - (7) without the source term using a two orders finite volume method.

- Secondly, we compute an approximation  $\rho_{si}^{n+2/3}$ ,  $\rho_a^{n+2/3}$ ,  $u^{n+2/3}$ ,  $E^{n+2/3}$ ,  $\phi^{n+2/3}$  and  $T_g^{n+2/3}$  adding the source term via an ordinary differential equation.

- The main point is to define  $\bar{H}^{n+2/3}$  in the gas using  $E^{n+2/3}$  and  $u^{n+2/3}$  to take into account the convection effect. In the solid, we take  $\bar{H}^{n+2/3} = \bar{H}^n$ . We then solve the heat equation in the whole domain to obtain  $\bar{H}^{n+1}$  using a finite volume method.

- At the moment  $\bar{H}^{n+1}$  is not homogeneous in the gas phase due to the diffusion process. Therefore, we compute a new  $E^{n+1}$  using an average of  $\bar{H}^{n+1}$  following y-direction in the gas and  $u^{n+2/3}$  to take the heat transfer into account.

- We finally obtain all the variables at time  $t^{n+1}$ .

#### 3.1. The heat equation resolution

To obtain a numerical approximation of the heat transfer, we use a finite volume scheme [4]. We introduce a bidimensional mesh compounded of rectangular cells. The computation is built on an implicit finite volume scheme. Indeed an explicit scheme leads to very small time step to satisfy the stability condition and yields to non reasonable computation time. The implicit formulation is given by:

$$\rho_v c_v \bar{T}_i^{n+1} = \rho_v c_v \bar{T}_i^n + \frac{\Delta t}{\Delta x} (F_1^{n+1} - F_3^{n+1}) + \frac{\Delta t}{\Delta y} (F_2^{n+1} - F_4^{n+1}) \quad (9)$$

where  $F_1$ ,  $F_2$ ,  $F_3$  and  $F_4$  represent the numerical fluxes at the cell interfaces using a centred difference scheme. The equation is rewritten in the matricial form:

$$A \cdot \bar{T}^{n+1} = B(\bar{T}^n)$$

where  $A$  is a symmetric matrix for a rectangular mesh. We obtain  $\bar{T}^{n+1}$  solving the linear system Eq. (9) by a conjugated gradient method.

#### 3.2. The convection model resolution

In order to obtain an approximate solution of the gas flow model in porous media, we use a fractional step technique [6]: on the one hand we solve separately during a small time step  $\Delta t$  the homogeneous conservative system, and on the other hand the right-hand side terms. Let  $U^n$  (conservative variable) be an approximation of  $U$  ( $t^n$ ) at time  $t^n$ . In order to obtain an approximation of  $U$  ( $t^{n+1}$ ) at time  $t^{n+1}=t^n+\Delta t$ , we first determine an approximate solution of the homogeneous problem using the finite volume scheme of the form:

$$\tilde{U}_i^{n+1} = U_i^n - \frac{\Delta t}{\Delta x} (F_{i+1/2}^n - F_{i-1/2}^n) \quad (10)$$

where  $F_{i+1/2}^n$  and  $F_{i-1/2}^n$  represent respectively the numerical fluxes calculated at the interface cells  $x = x_{i+1/2}$  and  $x = x_{i-1/2}$  using Roe method. Assumed now that  $\tilde{U}^{n+1}$  is the approximated solution value at  $t=t^{n+1}$  of the previous homogeneous problem, we solve the ordinary differential equation. Numerically, we add the right hand side contribution using a fourth-order explicit Runge-Kutta method.

### 4. The fuse domain geometry

The Fig. 2 represents the fuse domain used for the 1D 2D coupled models. The x-direction represents the gas flow direction for a fuse of length  $L=20$  mm and the y-direction represents a sand grain and the pore for evaluate the thermal exchanges. During the pre-arc period, the energy is injected in the solid and when the electrical arc is initiated, the energy is injected in the arc plasma.

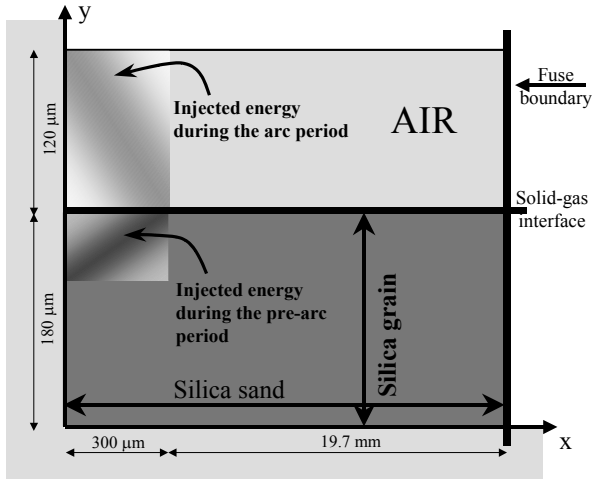


Fig. 2: Geometry of the fuse domain following x-direction and microscopic description of a silica grain following y-direction.

## 5. Numerical results and discussion

We present a simulation of an electrical arc discharge through a porous medium using realistic physical parameters for the silica sand. At the initial time, the system is at rest, the gas presents in the silica sand interstices is at atmospheric pressure and ambient temperature. Computations have been performed using the C++ finite volume library OFELI [7].

We present the plasma pressure evolution during the fuse operation and the mechanical granular pressure measured by piezoelectric pressure transducer at two positions (9 mm and 17 mm) in Fig. 3.

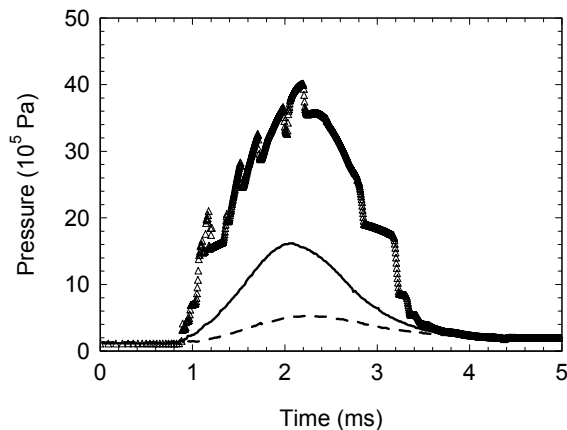


Fig. 3: Evolution of the plasma pressure versus time ( $\Delta$ ). The solid and the dash lines represent respectively the granular pressure measured at 9 and 17 mm of the arc column.

The plasma pressure increases up gradually to the maximum value which falls nearly on the same time of the maximum electric power. We note that the three profiles have the same evolution, during the discharge the arc plasma induces a stress effect on the peripheral grains.

The Fig. 4 represents a comparison of the plasma temperature evolution during the fuse operation between the numerical simulation and the spectroscopy [8].

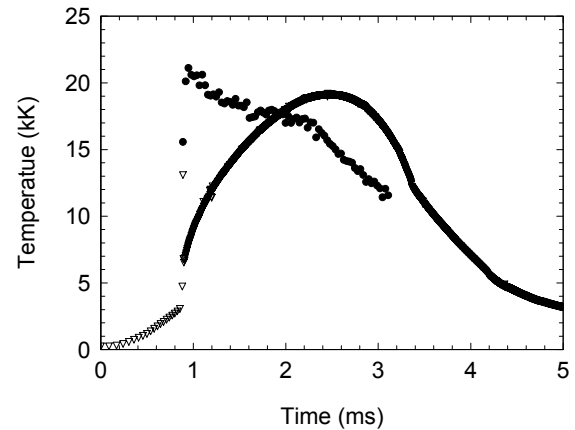


Fig. 4: Evolution of the plasma temperature versus time. The ( $\nabla$ ) and ( $\bullet$ ) represent respectively the numerical simulation and the spectroscopy.

We note that two maximums are the same order around 20000 K, but we have a difference on the profile evolution. Several explications can be formulated: the modelling represents the phenomenon following only one direction, the pre-arc period corresponding to the joule heating of the silver fuse element is approximated by a heating of the silica grains. Moreover the spectroscopy method integrates a 3D phenomenon.

The Fig. 5 and Fig. 6 represent respectively the gas pressure and the gas temperature evolution during the maximum of the injected energy ( $t=2.3$  ms) in the fuse domain. The phenomenon influences only the first 6-8 mm. The silica sand has absorbed the mechanical shock wave and the energy generated by the discharge. We can suppose that the 4-6 mm area is the preponderant area where takes place the fulgurite.

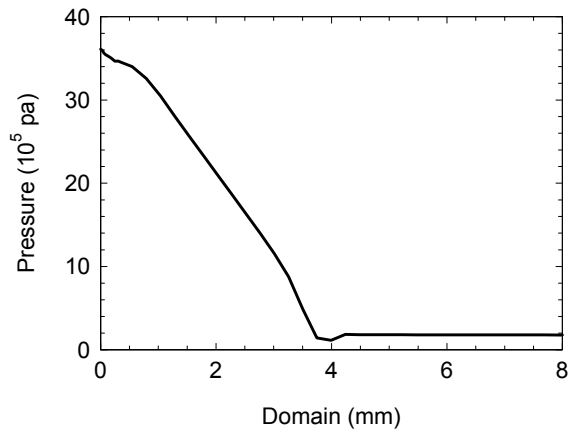


Fig. 5: Evolution of the gas pressure versus fuse domain at time  $t=2.3$  ms.

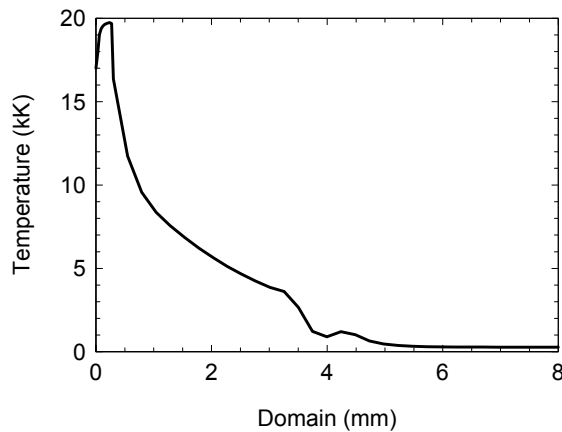


Fig. 6: Evolution of the gas temperature versus fuse domain at time  $t=2.3$  ms.

The Fig. 7 represents the thermal mapping of the silica sand at time  $t=2.3$  ms. The plasma pressure is evaluated around 20000 K.

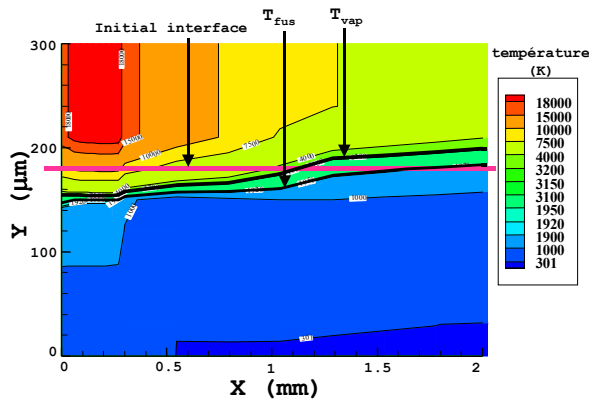


Fig. 7: Evolution of the solid and gas temperature versus fuse domain during the arc period  $t=2.3$  ms.

The first silica grains are partially vaporized and in a area farer, the silica vapour are recondensed at the contact with cold silica grains in comparing the vaporization isothermal with the initial solid-gas interface. Moreover, we note a liquid area evaluated by the vaporization and fusion isothermal.

In Fig. 8, we compare a fulgurite with the porosity evolution of the fuse domain. The porosity allows to show the evolution of the porous medium. The fulgurite is a combination of molten and vaporized fuse element metal and silica sand. In the first millimeters the porosity increases corresponding at the vaporization process and farer the porosity decreases corresponding to the silica sand vapour recondensed. We note that the areas of vaporization and recondensation are in according with the experimental fulgurite.

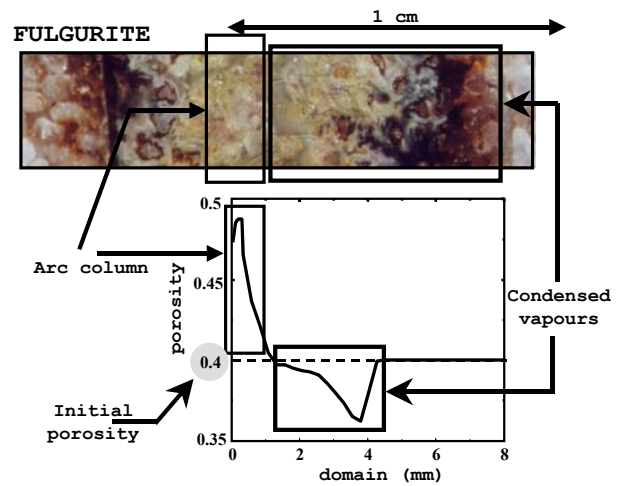


Fig. 8: Comparison of the fulgurite and the porosity evolution of the silica sand.

#### 4. Conclusion

A compressible gas flow model in porous media using a microscopic description of the heat transfer between the plasma and the silica sand was developed. The convection model based on the homogenized equations at two species in porous media takes into account the mechanical interaction due to the porous medium and the thermal model based on the total energy conservation allows to evaluate the heat and mass transfer between the two phases.

The numerical simulation with realistic physical parameters for the silica sand used in industrial fuses gives a description of the pressure, temperature evolution during the fuse operation. We have observed that the high plasma pressure  $40 \times 10^5$  Pa is maintained due to the conjunction of a high temperature, the gas produced by vaporization and

the Forchheimer force. The model allows to evaluate the vaporized and recondensed areas in the fuse domain.

Future works will consist in realizing a more complete model in adding the silver species and the pre-arc period corresponding to the Joule heating of the silver element.

## Acknowledgements

We thank, both for their financial support and their help through many discussions, M. S. Melquiond and X. Godechot from Alstom, M. Vérité from E.D.F, M. T. Rambaud and J.L. Gelet from Ferraz-Shawmut, and M. C. Fiévet and F. Gentils from Schneider Electric.

## References

- [1] Saquib M.A., Stokes A.D., "Characteristics of fuse arcing in different fillers". *ICEFA* Turin 1999, p. 275.
- [2] Bussière W., "Influence of sand granulometry on electrical characteristics, temperature and electron density during high-voltage fuse arc extinction", *J. Phys. D: Appl.Phys.*, 34, pp 925-935, 2001.
- [3] Bouddour A., Auriault J. L., Mhamdi-Aloui M., Bloch J. F., "Heat and mass transfer in wet porous media in presence evaporation-condensation", *Int. J. Heat Mass Transfer*, Vol 41, No 15, 2263-77, 1998.
- [4] Rochette D, "Modélisation et simulation de la décharge d'arc électrique dans un fusible moyenne tension", Ph.D Thesis (in french), Blaise Pascal University.
- [5] Jiang P.X., Ren Z.P., "Numerical investigation of forced convection heat transfer in porous media using a thermal non-equilibrium model", *International Journal of Heat and Fluid Flow*, 22, 102-110, 2001.
- [6] Toro E.F., "Riemann Solvers and Numerical Methods for Fluid Dynamics", Springer-Verlag, Berlin.
- [7] Touzani R., Object Finit Element Library OFELI, Copyright © 1998-2001.
- [8] Bussière W., "Mesure des grandeurs (T, N<sub>e</sub>, P) au sein du plasma d'arc des fusibles en moyenne tension », Ph.D Thesis (in french), Blaise Pascal University.